


**Interaction-induced transition in quantum many-body detection probability**Archak Purkayastha<sup>1,2,\*</sup> and Alberto Imparato<sup>3,†</sup><sup>1</sup>*Department of Physics, Indian Institute of Technology, Hyderabad 502284, India*<sup>2</sup>*Centre for Complex Quantum Systems, Aarhus University, Nordre Ringgade 1, 8000 Aarhus C, Denmark*<sup>3</sup>*Department of Physics and Astronomy, Aarhus University, Ny Munkegade, 8000 Aarhus C, Denmark* (Received 6 June 2023; revised 23 January 2024; accepted 31 January 2024; published 23 February 2024)

With the advent of digital and analog quantum simulation experiments, it is now possible to experimentally simulate the dynamics of quantum many-body lattice systems and make site-resolved measurements. These experiments make it pertinent to consider the probability of getting any specific measurement outcome, which we call the signal, on placing multiple detectors at various sites while simulating the dynamics of a quantum many-body lattice system. In this work we formulate and investigate this problem, introducing the concept of quantum many-body detection probability (QMBDP), which refers to the probability of detecting a chosen signal at least once in a given time. We show that, on tuning some Hamiltonian parameters, there can be sharp transition from a regime where the QMBDP is approximately equal to one to a regime where the QMBDP is approximately equal to zero. Most notably, the effects of such a transition can be observed at a single trajectory level. This is not a measurement-induced transition, but rather a nonequilibrium transition reflecting opening of a specific type of gap in the many-body spectrum. We demonstrate this in a single-impurity nonintegrable model, where changing the many-body interaction strength brings about such a transition. Our findings suggest that instead of measuring expectation values, single-shot stroboscopic measurements could be used to observe nonequilibrium transitions.

DOI: [10.1103/PhysRevA.109.L020202](https://doi.org/10.1103/PhysRevA.109.L020202)

*Introduction.* A fundamental question relevant across various branches of science is whether a chosen type of signal can be detected at a given position. One of the oldest mathematical formulations of the problem concerns a particle undergoing a random walk. The seminal Pólya's theorem [1] states that in one and two dimensions, the particle will eventually be detected with certainty regardless of the position of the detector, while in three dimensions there is a finite chance that the particle is never detected. Similar questions have been extensively studied in complex classical stochastic systems under the guise of survival and first-passage probabilities [2,3]. In the realm of quantum systems, these questions have been considered from the perspective of time-of-arrival and quantum search problems [4–23]. Most of these studies have primarily focused on single-particle systems with a single detector placed at a given location. Over the past decade, digital and analog quantum simulation experiments [24–28] have been developed to simulate the dynamics of quantum many-body lattice systems and make site-resolved measurements, for example, with quantum gas microscopes [29–45]. The advent of these experiments makes it pertinent to consider the detection probability of a signal in the presence of quantum many-body interactions, with multiple detectors placed at different lattice sites. In this paper we formulate and investigate this problem, providing an interesting example.

We define the signal as a particular measurement outcome of simultaneous stroboscopic projective measurements by the

detectors. We introduce the notion of quantum many-body detection probability (QMBDP), by which we refer to the probability that the signal is detected at least once within a given time. Choosing a single-impurity nonintegrable model [46–50], we demonstrate that, depending on initial state, there can be a sharp transition in QMBDP over a finite but large regime of time. In our chosen model, such a transition is brought about by tuning the many-body interaction strength. This transition is from a regime where the signal is almost certainly detected (QMBDP approximately equal to one) to a regime where the signal almost certainly is not detected (QMBDP approximately equal to zero). This is not a class of measurement-induced phase transition [51–54]. Instead, as we show in general, such a transition is related to opening a specific type of gap in the many-body spectrum of the system. It can be explained via an unconventional application of van Vleck perturbation theory (VVPT). It also manifests in far-from-equilibrium dynamical properties in the absence of the detectors, for example, in domain-wall dynamics. However, we find that the transition in QMBDP is much sharper than that in other dynamical properties. Most interestingly, since QMBDP takes into account the effects of measurement backaction, a transition in QMBDP can be captured at a single trajectory level. This opens the possibility of observing nonequilibrium transitions via single-shot stroboscopic measurements, rather than via obtaining dynamics of expectation values. This fact is both fundamentally interesting and experimentally appealing, with potential technological implications.

*Introducing QMBDP and our example.* Consider a quantum many-body lattice system with Hilbert space dimension  $D$  in a state far from equilibrium. Suppose that some

\*archak.p@phy.iith.ac.in

†imparato@phys.au.dk

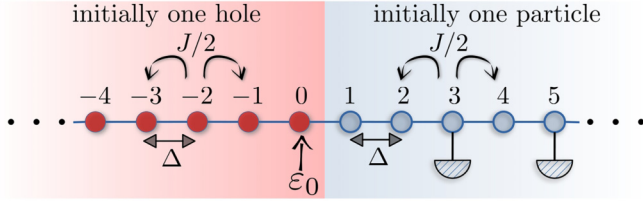


FIG. 1. We consider the Hamiltonian  $\hat{H} = -\sum_{\ell=-N/2+1}^{N/2-1} [\frac{J}{2}(\hat{c}_\ell^\dagger \hat{c}_{\ell+1} + \hat{c}_{\ell+1}^\dagger \hat{c}_\ell) + \Delta \hat{n}_\ell \hat{n}_{\ell+1}] + \varepsilon_0 \hat{n}_0$ , where  $\hat{c}_\ell$  is the fermionic annihilation operator at site  $\ell$  and  $\hat{n}_\ell = \hat{c}_\ell^\dagger \hat{c}_\ell$ . Initially the left half has only one hole, while the right site has only one particle. Two detectors are placed making simultaneous stroboscopic projective measurements of particle numbers at sites  $p$  and  $q$  (here  $p = 3$  and  $q = 5$ ) in intervals of time  $\tau$ . The signal is simultaneous detection on both detectors, with the projection operator  $\hat{P} = \hat{n}_p \hat{n}_q$ .

detectors are placed at some specific sites, which are switched on in stroboscopic steps of time  $\tau$ . The detectors make instantaneous projective measurement of some observable, say, particle number, in those sites. In this situation, one can ask about the probabilities of making a chosen type of observation. For example, if there are two particle detectors, one can ask what the probability is that they click simultaneously. We can think of the chosen type of observation as the signal. Let the Hamiltonian for the lattice system be  $\hat{H}$ , the initial state be  $\hat{\rho}(0)$ , the projection operator corresponding to measurement of the signal be  $\hat{P}$ , and the complementary projection operator be  $\hat{Q} = \hat{\mathbb{I}} - \hat{P}$ , where  $\hat{\mathbb{I}}$  is the identity operator. Using the Born rule and a little algebra, the probability of not detecting the signal in  $n$  steps is

$$R_n(\tau) = \text{Tr}\{[\hat{M}_Q(\tau)]^n \hat{A}(\tau) \hat{\rho}(0) \hat{A}^\dagger(\tau) [\hat{M}_Q^\dagger(\tau)]^n\}, \quad (1)$$

where  $\hat{M}_Q(\tau) = \hat{Q} e^{-i\hat{H}\tau} \hat{Q}$  and  $\hat{A}(\tau) = \hat{Q} e^{-i\hat{H}\tau} \hat{P} + \hat{M}_Q(\tau)$ . We call  $R_n(\tau)$  no-detection probability. This is the analog of the survival probability studied in classical stochastic systems [2,3]. The QMBDP, i.e., the probability that the signal is detected at least once within time  $n\tau$ , is given by  $T_n(\tau) = 1 - R_n(\tau)$ .

As a concrete example, we consider the model Hamiltonian described and schematically shown in Fig. 1. With  $\varepsilon_0 = 0$ , this Hamiltonian can be Jordan-Wigner transformed into the integrable  $XXZ$  qubit chain. With  $\varepsilon_0 > 0$ , the model becomes the nonintegrable single-impurity  $XXZ$  chain [48,49,55], which has been of interest recently because, despite being nonintegrable, it inherits the ballistic transport of the integrable  $XXZ$  chain for  $\Delta < J$  at high temperatures [47,49].

We divide the chain into left and right halves, the left half consisting of sites  $-N/2 + 1$  to 0 and the right half consisting of the remaining sites. We consider the case where, initially, there is only one hole (i.e., there are  $N/2 - 1$  particles) on the left half of the chain, while there is only one particle on the right half of the chain (see Fig. 1). Note that this does not correspond to a single configuration. The exact form of initial state will be discussed later. We put two detectors on the right half, at sites two arbitrary sites  $p$  and  $q$ ,  $p, q > 0$ , at a finite distance from the middle. They make simultaneous projective measurements of particle number in intervals of  $\tau$ . We take simultaneous detection at the two sites as our

signal. The corresponding projection operator is  $\hat{P} = \hat{n}_p \hat{n}_q$ , so  $\hat{Q} = \hat{\mathbb{I}} - \hat{n}_p \hat{n}_q$ .

*Physics governed by  $\hat{M}_Q(\tau)$ .* From Eq. (1) we see that the physics of QMBDP is governed by spectral properties of  $\hat{M}_Q(\tau)$ . The no-detection probability  $R_n(\tau)$  is bounded from above by 1. So the spectral radius of  $\hat{M}_Q(\tau)$ , i.e., the highest magnitude of its eigenvalues, must be less than or equal to 1. Consequently, in complete generality, we can write the eigenvalues of  $\hat{M}_Q(\tau)$  as  $\{e^{-\lambda_m(\tau) + i\theta_m(\tau)}\}$ , with  $\lambda_m \geq 0$ ,  $\theta_m$  being real,  $m$  going from 1 to  $D_Q$ , where  $D_Q < D$  is the Hilbert space dimension of the  $\hat{Q}$  subspace.

Let the eigenvalues of  $\hat{M}_Q(\tau)$  be arranged in ascending order of  $\lambda_m(\tau)$ . Then we immediately see that for  $\lambda_1(\tau) > 0$ , i.e., when the spectral radius is smaller than unity, if  $n \gg 1/\lambda_1(\tau)$ , the signal is almost certainly detected, irrespective of the initial state. Thus,  $\tau/\lambda_1(\tau)$  gives the timescale for certainly detecting the signal. It is crucial to note that this finite timescale for certainly detecting the signal irrespective of the initial state arises due to repeated stroboscopic measurements and has no analog in the absence of such measurements.

An interesting case arises if  $\hat{M}_Q(\tau)$  has unit spectral radius, i.e.,  $\lambda_1(\tau) = 0$ . In this case, depending on whether the initial state has substantial overlap with the corresponding eigenvector of  $\hat{M}_Q(\tau)$ , there is a finite probability that the signal is never detected. For arbitrary finite  $\tau$ , this condition can happen if and only if some eigenvectors of  $\hat{H}$  belong entirely to the  $\hat{Q}$  subspace, i.e., are simultaneous eigenvectors of  $\hat{Q}$  with eigenvalue 1 [56]. Let the number of such eigenvectors be  $D'_Q, D'_Q \leq D_Q$ , and the projection operator onto this subspace be  $\hat{Q}'$ . Then  $\hat{H}$  can be block diagonalized as

$$\hat{H} = \hat{Q}' \hat{H} \hat{Q}' + \hat{P}' \hat{H} \hat{P}', \quad \hat{P}' = \hat{\mathbb{I}} - \hat{Q}'. \quad (2)$$

If the initial state belongs to  $\hat{Q}'$  subspace, the Hamiltonian dynamics does not take it outside of this subspace and hence the signal will never be detected. This is irrespective of the value of  $\tau$ . This understanding lets us relate the unit spectral radius of  $\hat{M}_Q(\tau)$  to specific spectral gaps in the Hamiltonian.

*Relation with spectral gaps of the Hamiltonian.* Let  $\hat{H} = \hat{H}_0 + \hat{H}_1$ , where  $\hat{H}_0$  is a simpler Hamiltonian, whose spectral properties are easily accessible, and  $\hat{H}_1$  acts as a perturbation on it. In particular, we consider a situation where  $D_{Q_0}$ , the number of eigenvectors of  $\hat{H}_0$ , is known to completely belong to  $\hat{Q}$  subspace, with  $D_{Q_0} \leq D_Q$ . Let  $\hat{Q}_0$  be the projection operator for this subspace. We have the block-diagonal structure  $\hat{H}_0 = \hat{Q}_0 \hat{H}_0 \hat{Q}_0 + \hat{P}_0 \hat{H}_0 \hat{P}_0$ ,  $\hat{P}_0 = \hat{\mathbb{I}} - \hat{Q}_0$ . The Hamiltonian  $\hat{H}_1$  mixes the two subspaces, but has no component completely within the  $\hat{Q}_0$  subspace. The question is, with above assumptions, under what condition a similar block diagonalization can be approximately preserved in the presence of  $\hat{H}_1$ .

The answer is succinctly provided by VVPT. Let  $|E_\alpha^{Q_0}\rangle$  be the eigenstate of  $\hat{H}_0$  in  $\hat{Q}_0$  subspace with energy  $E_\alpha^{Q_0}$  and  $|E_\nu^{P_0}\rangle$  be the eigenstate of  $\hat{H}_0$  in  $\hat{P}_0$  subspace with energy  $E_\nu^{P_0}$ . Equation (2) is approximately satisfied if for some range of  $\alpha \in \{\alpha_{\min}, \alpha_{\max}\}$  the eigenstates of  $\hat{H}_0$  in  $\hat{Q}_0$  subspace are energetically gapped from those of  $\hat{P}_0$  subspace in the sense

$$g_\alpha := \max_\nu \left| \frac{\langle E_\alpha^{Q_0} | \hat{H}_1 | E_\nu^{P_0} \rangle}{E_\alpha^{Q_0} - E_\nu^{P_0}} \right| \ll 1, \quad \alpha \in \{\alpha_{\min}, \alpha_{\max}\}. \quad (3)$$

Let the number of such eigenstates be  $D'_0 \leq D_{Q_0}$  and  $\hat{Q}'$  be the projection operator onto this subspace. Under such conditions, starting with  $\hat{H}$  written in the eigenbasis of  $\hat{H}_0$ , van Vleck perturbation theory gives a systematic way to perturbatively find a unitary operator  $\hat{U}_r$  to  $r$ th order such that  $\hat{U}_r^\dagger \hat{H} \hat{U}_r = \hat{H}^{(r)}$  is approximately block diagonal, i.e.,  $\hat{H}^{(r)} \simeq \hat{Q}' \hat{H}^{(r)} \hat{Q}' + \hat{P}' \hat{H}^{(r)} \hat{P}'$ , with  $\hat{P}' = \hat{1} - \hat{Q}'$  [57,58]. On further diagonalizing  $\hat{H}^{(r)}$  the two subspaces mix only a little. It follows that Eq. (2) is satisfied to a good approximation.

In our example, we choose  $\hat{H}_1 = -\frac{J}{2}(\hat{c}_1^\dagger \hat{c}_0 + \hat{c}_0^\dagger \hat{c}_1)$ , i.e., just the hopping term between the left and right halves. Then  $\hat{H}_0 = \hat{H} - \hat{H}_1$  is the Hamiltonian without this hopping term. Without this hopping, the numbers of particles in the left ( $N_L$ ) and right ( $N_R$ ) halves are separately conserved. Let us restrict the discussion to the half-filling case  $N_L + N_R = N/2$  so that  $N_R$  is the only remaining quantum number. We immediately see that our choice of initial condition belongs to  $N_R = 1$  sector of  $\hat{H}_0$ . We take the initial state as an energy filtered random state in this sector of  $\hat{H}_0$ ,

$$|\psi(0)\rangle \propto \exp\left[-\left(\frac{\hat{H}_0 - E}{\sigma}\right)^2\right] |\psi_{\text{rand}}\rangle_{N_R=1}, \quad (4)$$

where the  $|\psi_{\text{rand}}\rangle_{N_R=1}$  is a randomly chosen state in  $N_R = 1$  sector and the prefactor is a Gaussian filter peaked around energy  $E$  with a standard deviation  $\sigma$ .

Since our signal is detecting two particles simultaneously in the right half, we define  $\hat{Q}_0$  as the projector onto  $N_R = 0, 1$  sectors. Our choice of initial state belongs to the  $\hat{Q}_0$  subspace. It is also clear that  $\hat{H}_1$  connects  $N_R$  and  $N_R + 1$  sectors. Therefore, to evaluate Eq. (3), we only need to diagonalize  $\hat{H}_0$  in  $N_R = 1$  and  $N_R = 2$  subspaces. The Hilbert space dimensions of  $N_R = 1$  and  $N_R = 2$  subspaces of  $\hat{H}_0$  scale as  $N^2$  and  $N^4$ , respectively, which are far smaller than exponential scaling of the Hilbert space dimension of the full  $\hat{H}$  in the half-filling sector.

In Fig. 2(a) we plot  $g_\alpha$  as a function of  $\Delta$ , for various values of  $\alpha$ . We have arranged the eigenstates in  $\hat{Q}_0$  subspace such that  $\alpha = 0$  corresponds to  $N_R = 0$ , which is just one configuration, and  $\alpha \geq 1$  are the eigenstates in  $N_R = 1$  sector in ascending order of energy. In Fig. 2(a) we see that for the lowest few eigenstates in  $N_R = 1$  sector,  $g_\alpha \ll 1$  when  $\Delta > J$ , while this is not the case for  $\Delta < J$ . Contrarily, for a mid-spectrum state  $\alpha = \alpha_{\text{mid}} = \lceil D_{Q_0}/2 \rceil$ , we find  $g_\alpha > 1 \forall \Delta$ . Thus, we see clear evidence that Eq. (3) is satisfied in a low-energy range when  $\Delta > J$ , while for  $\Delta < J$ , it is not satisfied. It is interesting to note that, although the Hamiltonian parameters  $J$ ,  $\Delta$ , and  $\varepsilon_0$  are of the same order,  $g_\alpha$  emerges as a perturbative parameter for VVPT in the low-energy regime when  $\Delta > J$ .

*Transition in detection probability.* Given that we have a situation where on changing a parameter in  $\hat{H}_0$  across some value an energy gap opens between some eigenstates in  $\hat{Q}_0$  subspace and those of  $\hat{P}_0$  subspace in the sense of Eq. (3), it is now clear that this will lead to a sharp decrease in  $\lambda_1(\tau)$ . Indeed, such a sharp decrease in  $\lambda_1(\tau)$  on tuning  $\Delta/J$  across 1 is clearly seen in Fig. 2(b). In terms of the nonunitary matrix  $\hat{M}_Q(\tau)$ , this change in  $\lambda_1(\tau)$  is reminiscent of gap closing in a quantum transition. Physically, the transition is from a regime

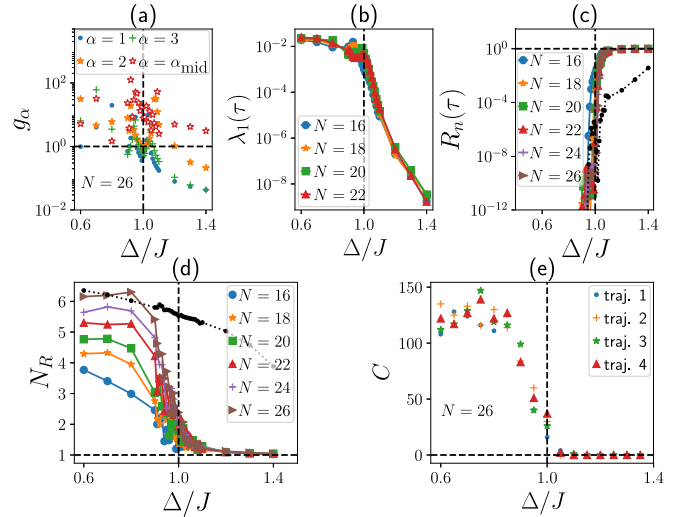


FIG. 2. (a) Plot of  $g_\alpha$  [see Eq. (3)] with  $\Delta$  for various values of  $\alpha$ . Here  $\alpha_{\text{mid}} = \lceil D_{Q_0}/2 \rceil$  and  $N = 26$ . (b) Plot of  $\lambda_1(\tau)$  with  $\Delta$ , for various system sizes and  $\tau = 2J^{-1}$ . (c) Plot of no-detection probability  $R_n(\tau)$  with  $\Delta$  after  $n = 1000$  steps. (d) Plot of  $N_R$  with  $\Delta$  at time  $n\tau = 2000J^{-1}$  in the absence of any detector. For the symbols in (c) and (d) the initial state is of the form in Eq. (4) with  $E = E_1^{Q_0}$ . The dots in (c) and (d) are the corresponding plots starting from a different initial state with  $E = E_{\alpha_{\text{mid}}}^{Q_0}$  and system size  $N = 26$ . (e) Number of times the signal  $C$  is detected in  $n = 1000$  steps in individual runs of the experiment starting with the initial state of the form in Eq. (4) with  $E = E_1^{Q_0}$ , plotted as a function of  $\Delta$ . The plot shows results for four different runs (trajectories). The transition at the single trajectory level is clear. The other parameters are  $\varepsilon_0 = 0.5J$ ,  $\sigma = 0.1J$ , and detector sites  $p = 3$  and  $q = 5$ . The numerical techniques used to obtain the data are (a) exact diagonalization and (b) Arnoldi iteration [59,60] with sparse matrix methods [56], which was computationally possible up to  $N = 22$  (Hilbert space dimension  $D = 705\,432$ ). The time evolutions required for (b)–(e) were done with the Chebyshev polynomial method [61–64] with a sparse matrix, which was computationally possible up to  $N = 26$  ( $D = 10\,400\,600$ ).

where the signal is almost certainly detected in a finite time irrespective of the initial state (QMBDP approximately equal to one) to a where, depending on the initial state, it may not be detected (QMBDP approximately equal to zero), as we show next.

For large  $n$ , no-detection probability goes as  $R_n(\tau) \sim e^{-2\lambda_1 n}$  [see Eq. (1)]. So Fig. 2(b) then suggests that, if we start from an initial state of the form of Eq. (4) with  $E = E_1^{Q_0}$  and fix the number of steps  $n$  to be in the range  $10^2 \ll n \ll 10^4$ , which is finite but large, we should see a sharp transition in detection probability on tuning  $\Delta/J$  across 1. This is shown in Fig. 2(c), where we plot the corresponding  $R_n(\tau)$ , with  $n = 1000$ , as a function of  $\Delta/J$ . For all values of  $N$ ,  $R_n(\tau)$  shows an increase of more than 12 orders of magnitude on tuning  $\Delta/J$  from 0.9 to 1.1, reaching  $R_n(\tau) \approx 1$  for larger values. On increasing  $N$ , the transition becomes sharper, although the finite-size effect is small because the detectors are placed in the bulk of the system, at a finite distance from the middle.

It is tempting to explain this transition from the known fact that transport goes from ballistic to diffusive on going



across  $\Delta = J$  [50], which may cause particles from the left half to not reach the sites  $p$  and  $q$  within the chosen time. However, this would be inconsistent, because the sites  $p$  and  $q$  are chosen at a finite distance from the middle and the time  $n\tau = 2000J^{-1}$  should have been large enough to transport particles diffusively. Instead, our understanding in terms of VVPT consistently explains the phenomenon.

When we start with an initial state of the form of Eq. (4) with  $E = E_{\alpha_{\text{mid}}}^{Q_0}$ , we still see an exponential rise in  $R_n(\tau)$  on going across  $\Delta/J = 1$ , as shown by the dotted line in Fig. 2(c). This is because such a state also has a small overlap with the low-energy states of  $\hat{H}_0$ . Nevertheless, since mid-spectrum states of  $\hat{H}_0$  do not satisfy Eq. (3), as seen in Fig. 2(a),  $R_n(\tau) \ll 1$  even for  $\Delta/J > 1$  in this case, within the range of parameters considered.

*Relation to domain-wall melting.* On Jordan-Wigner transforming, our choice of initial state is akin to a domain wall in the sense that total magnetization of the left half (proportional to  $N_L - N/2$ ) is positive and that of the right half (proportional to  $N_R - N/2$ ) is negative. Our understanding in terms of VVPT is that, when starting from an initial state with  $E = E_1^{Q_0}$ , for  $\Delta > J$ , the Hamiltonian dynamics hardly takes the system out of  $N_R = 1$  subspace. Thus, in such a case, the initial domain wall “does not melt” up to a long time. Contrarily, for  $\Delta < J$ , the particles should be evenly distributed between left and right halves, as expected in a generic system. So the domain wall should melt.

This is clearly seen in Fig. 2(d), where we show plots of the number of particles on the right half  $N_R$  at time  $n\tau$  in the absence of any detectors, i.e., for continuous time evolution with the system Hamiltonian. Thus, even in the absence of any measurement, there is a transition in nonequilibrium dynamics on tuning  $\Delta$  across  $J$ . However, this transition is not as sharp as that in  $R_n(\tau)$ . Nevertheless, since we find  $N_R \sim 1$  for  $\Delta > J$ , Fig. 2(d) establishes that putting detectors at any two sites on right half and choosing any finite value of  $\tau$  would lead to a similar transition in  $R_n(\tau)$ .

Consistently with VVPT, when starting from the initial state with  $E = E_{\alpha_{\text{mid}}}^{Q_0}$ , we find that  $N_R$  decreases smoothly with  $\Delta$  with no hint of any transition, as shown by the dotted line in Fig. 2(d). Thus, in this case, the domain wall melts for all values of  $\Delta/J$  within the observed time. This is interesting because in terms of magnetization of the left and right halves, there is no difference between the two initial states with  $E = E_{\alpha_{\text{mid}}}^{Q_0}$  and  $E = E_1^{Q_0}$ . The physics of domain wall melting was previously explored in the single-impurity nonintegrable system in only one work [46], although it has been extensively studied for integrable  $XXZ$  chains [65–71].

*Transition at the single trajectory level.* Our understanding of the transition in terms of  $\hat{M}_Q(\tau)$  shows that, irrespective of the initial state, after every approximately  $1/\lambda_1(\tau)$  stroboscopic measurements, the signal is detected. Let  $C$  be the number of times the signal is detected in  $n$  steps in a single run of the experiment. Note that  $C$  is a stochastic variable, in general having different values for each run of the experiment. However, by the above argument, if  $n \gg 1/\lambda_1(\tau)$ , which implies  $R_n(\tau) \ll 1$ , we expect a large value of  $C$ . Contrarily, if  $R_n(\tau) \sim 1$ , we expect a small value of  $C$ . Therefore, we find that a transition corresponding to that in  $R_n(\tau)$  will be seen

in terms of  $C$  at a single trajectory level. This is confirmed in Fig. 2(e), where we show results for four trajectories obtained from Monte Carlo simulation [56].

This is remarkable since observing far-from-equilibrium transitions in quantum systems usually requires measurement of expectation values as a function of time. To measure expectation values at a chosen time point for a given set of system parameters, one requires averaging over measurement outcomes of several identical runs of the experiment. Each run includes preparing the initial state, evolving up to the chosen time point and making the measurement. Then, to obtain expectation values at the next time point, the entire process has to be repeated. Finally, the whole set of steps needs to be repeated for several values of system parameters to obtain the transition. Fundamentally, the requirement of having several such identical runs for each time point stems from the need to avoid effects of measurement backaction while obtaining expectation values. Instead, a transition in QMBDP takes into account the effects of measurement backaction. Consequently, as shown in Fig. 2(e), the above transition can be seen by counting the number of simultaneous clicks in the two detectors in one single run of the experiment for each value of  $\Delta/J$ . This is certainly experimentally more appealing than observing the transition via the dynamics of expectation values.

This also has potential technological implications. A transition in QMBDP might be useful in quantum Hamiltonian learning and parameter estimation [72–79]. For example, in our setting, if  $\Delta$  is unknown but  $J$  is tunable, running the experiment only once for every value of  $J$  over a wide enough range,  $\Delta$  can be estimated, since the transition occurs at the single trajectory level at  $\Delta = J$ . No ensemble averaging would be required for this. Detailed exploration of such applications of transitions in QMBDP is beyond the scope of the present paper and is left for future work.

*Conclusion.* The physics of QMBDP, which we introduced and explored in this work, is experimentally relevant and of both fundamental and technological interest. It brings together several ideas from seemingly disparate fields, such as statistical physics of stochastic systems, quantum measurements, and quantum many-body physics, and opens the possibility of observing nonequilibrium transitions via single-shot stroboscopic measurements. Quantum simulation experiments [24–28] are ideal platforms to test our results. We have numerically explored one interesting example. However, the general formulation of QMBDP in Eq. (1) and its relation to many-body spectral gaps in the sense of Eq. (3) are valid for arbitrary Hamiltonians and projection operators that define the signal. This provides the framework for future research exploring possible transitions in QMBDP in other systems and geometries, as well as for various types of signals.

*Acknowledgments.* We are grateful to Klaus Mølmer and Eli Barkai for helpful discussions. A.P. acknowledges funding from the Danish National Research Foundation through the Center of Excellence CCQ (Grant Agreement No. DNRF156) and Seed Grant from IIT Hyderabad, Project No. SG/IITH/F331/2023-24/SG-169. A.P. acknowledges the Grendel supercomputing cluster at Aarhus University, where many of the calculations were done. A.P. also thanks

Anupam Gupta at Indian Institute of Technology, Hyderabad, for giving access to his workstation where some of the calculations were carried out. We also thank the

anonymous referees for their comprehensive reviews and constructive criticism, which substantially improved the paper.

- 
- [1] G. Pólya, *Math. Ann.* **84**, 149 (1921).
- [2] A. J. Bray, S. N. Majumdar, and G. Schehr, *Adv. Phys.* **62**, 225 (2013).
- [3] S. Redner, [arXiv:2201.10048](https://arxiv.org/abs/2201.10048).
- [4] M. Kulkarni and S. N. Majumdar, *J. Phys. A: Math. Theor.* **56**, 385003 (2023).
- [5] Q. Liu, D. A. Kessler, and E. Barkai, *Phys. Rev. Res.* **5**, 023141 (2023).
- [6] Q. Liu, K. Ziegler, D. A. Kessler, and E. Barkai, *Phys. Rev. Res.* **4**, 023129 (2022).
- [7] Q. Liu, R. Yin, K. Ziegler, and E. Barkai, *Phys. Rev. Res.* **2**, 033113 (2020).
- [8] V. Dubey, C. Bernardin, and A. Dhar, *Phys. Rev. A* **103**, 032221 (2021).
- [9] F. Thiel, I. Mualem, D. Kessler, and E. Barkai, *Entropy* **23**, 595 (2021).
- [10] F. Thiel, I. Mualem, D. Meidan, E. Barkai, and D. A. Kessler, *Phys. Rev. Res.* **2**, 043107 (2020).
- [11] F. Thiel, I. Mualem, D. A. Kessler, and E. Barkai, *Phys. Rev. Res.* **2**, 023392 (2020).
- [12] R. Yin, K. Ziegler, F. Thiel, and E. Barkai, *Phys. Rev. Res.* **1**, 033086 (2019).
- [13] F. Thiel, E. Barkai, and D. A. Kessler, *Phys. Rev. Lett.* **120**, 040502 (2018).
- [14] H. Friedmann, D. A. Kessler, and E. Barkai, *J. Phys. A: Math. Theor.* **50**, 04LT01 (2017).
- [15] S. Chakraborty, L. Novo, A. Ambainis, and Y. Omar, *Phys. Rev. Lett.* **116**, 100501 (2016).
- [16] S. Dhar, S. Dasgupta, A. Dhar, and D. Sen, *Phys. Rev. A* **91**, 062115 (2015).
- [17] S. Dhar, S. Dasgupta, and A. Dhar, *J. Phys. A: Math. Theor.* **48**, 115304 (2015).
- [18] F. A. Grünbaum, L. Velázquez, A. H. Werner, and R. F. Werner, *Commun. Math. Phys.* **320**, 543 (2013).
- [19] C. Anastopoulos and N. Savvidou, *Phys. Rev. A* **86**, 012111 (2012).
- [20] H. Krovi and T. A. Brun, *Phys. Rev. A* **74**, 042334 (2006).
- [21] E. Bach, S. Coppersmith, M. P. Goldschen, R. Joynt, and J. Watrous, *J. Comput. Syst. Sci.* **69**, 562 (2004).
- [22] J. A. Damborenea, I. L. Egusquiza, G. C. Hegerfeldt, and J. G. Muga, *Phys. Rev. A* **66**, 052104 (2002).
- [23] J. Muga and C. Leavens, *Phys. Rep.* **338**, 353 (2000).
- [24] F. Schäfer, T. Fukuhara, S. Sugawa, Y. Takasu, and Y. Takahashi, *Nat. Rev. Phys.* **2**, 411 (2020).
- [25] M. Morgado and S. Whitlock, *AVS Quantum Sci.* **3**, 023501 (2021).
- [26] C. Monroe, W. C. Campbell, L.-M. Duan, Z.-X. Gong, A. V. Gorshkov, P. W. Hess, R. Islam, K. Kim, N. M. Linke, G. Pagano, P. Richerme, C. Senko, and N. Y. Yao, *Rev. Mod. Phys.* **93**, 025001 (2021).
- [27] A. J. Daley, I. Bloch, C. Kokail, S. Flannigan, N. Pearson, M. Troyer, and P. Zoller, *Nature (London)* **607**, 667 (2022).
- [28] M. C. Tran, D. K. Mark, W. W. Ho, and S. Choi, *Phys. Rev. X* **13**, 011049 (2023).
- [29] W. S. Bakr, J. I. Gillen, A. Peng, S. Fölling, and M. Greiner, *Nature (London)* **462**, 74 (2009).
- [30] J. F. Sherson, C. Weitenberg, M. Endres, M. Cheneau, I. Bloch, and S. Kuhr, *Nature (London)* **467**, 68 (2010).
- [31] C. Gross and W. S. Bakr, *Nat. Phys.* **17**, 1316 (2021).
- [32] D. Wei, A. Rubio-Abadal, B. Ye, F. Machado, J. Kemp, K. Srakaew, S. Hollerith, J. Rui, S. Gopalakrishnan, N. Y. Yao, I. Bloch, and J. Zeiher, *Science* **376**, 716 (2022).
- [33] T. A. Hilker, G. Salomon, F. Grusdt, A. Omran, M. Boll, E. Demler, I. Bloch, and C. Gross, *Science* **357**, 484 (2017).
- [34] P. T. Brown, D. Mitra, E. Guardado-Sanchez, P. Schauß, S. S. Kondov, E. Khatami, T. Paiva, N. Trivedi, D. A. Huse, and W. S. Bakr, *Science* **357**, 1385 (2017).
- [35] L. W. Cheuk, M. A. Nichols, K. R. Lawrence, M. Okan, H. Zhang, E. Khatami, N. Trivedi, T. Paiva, M. Rigol, and M. W. Zwierlein, *Science* **353**, 1260 (2016).
- [36] M. Boll, T. A. Hilker, G. Salomon, A. Omran, J. Nespolo, L. Pollet, I. Bloch, and C. Gross, *Science* **353**, 1257 (2016).
- [37] M. F. Parsons, A. Mazurenko, C. S. Chiu, G. Ji, D. Greif, and M. Greiner, *Science* **353**, 1253 (2016).
- [38] D. Greif, M. F. Parsons, A. Mazurenko, C. S. Chiu, S. Blatt, F. Huber, G. Ji, and M. Greiner, *Science* **351**, 953 (2016).
- [39] P. M. Preiss, R. Ma, M. E. Tai, J. Simon, and M. Greiner, *Phys. Rev. A* **91**, 041602(R) (2015).
- [40] A. Omran, M. Boll, T. A. Hilker, K. Kleinlein, G. Salomon, I. Bloch, and C. Gross, *Phys. Rev. Lett.* **115**, 263001 (2015).
- [41] M. F. Parsons, F. Huber, A. Mazurenko, C. S. Chiu, W. Setiawan, K. Wooley-Brown, S. Blatt, and M. Greiner, *Phys. Rev. Lett.* **114**, 213002 (2015).
- [42] T. Fukuhara, S. Hild, J. Zeiher, P. Schauß, I. Bloch, M. Endres, and C. Gross, *Phys. Rev. Lett.* **115**, 035302 (2015).
- [43] E. Haller, J. Hudson, A. Kelly, D. A. Cotta, B. Peaudecerf, G. D. Bruce, and S. Kuhr, *Nat. Phys.* **11**, 738 (2015).
- [44] R. Islam, R. Ma, P. M. Preiss, M. Eric Tai, A. Lukin, M. Rispoli, and M. Greiner, *Nature (London)* **528**, 77 (2015).
- [45] M. Cheneau, P. Barmettler, D. Poletti, M. Endres, P. Schauß, T. Fukuhara, C. Gross, I. Bloch, C. Kollath, and S. Kuhr, *Nature (London)* **481**, 484 (2012).
- [46] L. F. Santos and A. Mitra, *Phys. Rev. E* **84**, 016206 (2011).
- [47] M. Brenes, E. Mascarenhas, M. Rigol, and J. Goold, *Phys. Rev. B* **98**, 235128 (2018).
- [48] M. Brenes, T. LeBlond, J. Goold, and M. Rigol, *Phys. Rev. Lett.* **125**, 070605 (2020).
- [49] M. Brenes, J. Goold, and M. Rigol, *Phys. Rev. B* **102**, 075127 (2020).
- [50] B. Bertini, F. Heidrich-Meisner, C. Karrasch, T. Prosen, R. Steinigeweg, and M. Žnidarič, *Rev. Mod. Phys.* **93**, 025003 (2021).
- [51] M. Buchhold, Y. Minoguchi, A. Altland, and S. Diehl, *Phys. Rev. X* **11**, 041004 (2021).

- [52] Q. Tang and W. Zhu, *Phys. Rev. Res.* **2**, 013022 (2020).
- [53] B. Skinner, J. Ruhman, and A. Nahum, *Phys. Rev. X* **9**, 031009 (2019).
- [54] S. Dhar and S. Dasgupta, *Phys. Rev. A* **93**, 050103(R) (2016).
- [55] L. F. Santos, *J. Phys. A: Math. Gen.* **37**, 4723 (2004).
- [56] See Supplemental Material at <http://link.aps.org/supplemental/10.1103/PhysRevA.109.L020202> for further proofs and plots.
- [57] I. Shavitt and L. T. Redmon, *J. Chem. Phys.* **73**, 5711 (1980).
- [58] C. Cohen-Tannoudji, J. Dupont-Roc, and G. Grynberg, *Atom-Photon Interactions: Basic Process and Applications* (Wiley-VCH, Weinheim, 2004).
- [59] W. E. Arnoldi, *Q. Appl. Math.* **9**, 17 (1951).
- [60] Z.-X. Jia and L. Elsner, *J. Comput. Math.* **18**, 265 (2000).
- [61] H. Tal-Ezer and R. Kosloff, *J. Chem. Phys.* **81**, 3967 (1984).
- [62] R. Chen and H. Guo, *Comput. Phys. Commun.* **119**, 19 (1999).
- [63] V. V. Dobrovitski and H. A. De Raedt, *Phys. Rev. E* **67**, 056702 (2003).
- [64] H. Fehske, J. Schleede, G. Schubert, G. Wellein, V. S. Filinov, and A. R. Bishop, *Phys. Lett. A* **373**, 2182 (2009).
- [65] G. Misguich, N. Pavloff, and V. Pasquier, *SciPost Phys.* **7**, 025 (2019).
- [66] O. Gamayun, Y. Miao, and E. Ilievski, *Phys. Rev. B* **99**, 140301(R) (2019).
- [67] G. Misguich, K. Mallick, and P. L. Krapivsky, *Phys. Rev. B* **96**, 195151 (2017).
- [68] J.-M. Stéphan, *J. Stat. Mech.* (2007) 103108.
- [69] J. Mossel and J.-S. Caux, *New J. Phys.* **12**, 055028 (2010).
- [70] S. Yuan, H. De Raedt, and S. Miyashita, *Phys. Rev. B* **75**, 184305 (2007).
- [71] D. Gobert, C. Kollath, U. Schollwöck, and G. Schütz, *Phys. Rev. E* **71**, 036102 (2005).
- [72] V. Gebhart, R. Santagati, A. A. Gentile, E. M. Gauger, D. Craig, N. Ares, L. Banchi, F. Marquardt, L. Pezzè, and C. Bonato, *Nat. Rev. Phys.* **5**, 141 (2023).
- [73] J. Yang, S. Pang, A. del Campo, and A. N. Jordan, *Phys. Rev. Res.* **4**, 013133 (2022).
- [74] S. Qin, M. Cramer, C. P. Koch, and A. Serafini, *SciPost Phys.* **13**, 121 (2022).
- [75] J. Wang, S. Paesani, R. Santagati, S. Knauer, A. A. Gentile, N. Wiebe, M. Petruzzella, J. L. O'Brien, J. G. Rarity, A. Laing, and M. G. Thompson, *Nat. Phys.* **13**, 551 (2017).
- [76] D. Burgarth and A. Ajoy, *Phys. Rev. Lett.* **119**, 030402 (2017).
- [77] H. Yuan and C.-H. F. Fung, *Phys. Rev. Lett.* **115**, 110401 (2015).
- [78] J. Zhang and M. Sarovar, *Phys. Rev. Lett.* **113**, 080401 (2014).
- [79] S. Pang and T. A. Brun, *Phys. Rev. A* **90**, 022117 (2014).